PAPER

Convex and Differentiable Formulation for Inverse Problems in Hilbert Spaces with Nonlinear Clipping Effects

Natsuki UENO[†a)], ***Nonmember***, **Shoichi KOYAMA**[†], ***and*** **Hiroshi SARUWATARI**[†], ***Members***

SUMMARY We propose a useful formulation for ill-posed inverse problems in Hilbert spaces with nonlinear clipping effects. Ill-posed inverse problems are often formulated as optimization problems, and nonlinear clipping effects may cause nonconvexity or nondifferentiability of the objective functions in the case of commonly used regularized least squares. To overcome these difficulties, we present a tractable formulation in which the objective function is convex and differentiable with respect to optimization variables, on the basis of the Bregman divergence associated with the primitive function of the clipping function. By using this formulation in combination with the representer theorem, we need only to deal with a finite-dimensional, convex, and differentiable optimization problem, which can be solved by well-established algorithms. We also show two practical examples of inverse problems where our theory can be applied, estimation of band-limited signals and time-harmonic acoustic fields, and evaluate the validity of our theory by numerical simulations.

key words: *inverse problem, Hilbert space, representer theorem, Bregman divergence, convex optimization*

1. Introduction

An inverse problem is a process of determining or estimating a quantity of interest from its indirect observation, called a forward problem, whose theory has been under intensive investigation in engineering, applied mathematics, and many other fields. Here, we consider the following types of forward problem:

$$s = (f_1(L_1 u), \ldots, f_N(L_N u)), \tag{1}$$

where N is a natural number, $u \in \mathcal{U}$ is a quantity of interest, $\mathcal{U}$ is a real Hilbert space consisting of all possible candidates for quantities of interest, $s \in \mathcal{S}$ is observed data, $\mathcal{S} \subseteq \mathbb{R}^N$ is a set consisting of all possible candidates for observed data, $L_1, \ldots, L_N : \mathcal{U} \to \mathbb{R}$ are bounded linear functionals, and $f_1, \ldots, f_N : \mathbb{R} \to \mathbb{R}$ are continuous and monotonically increasing (not necessarily strictly monotonically increasing and therefore not necessarily invertible) functions representing nonlinear clipping effects (hereafter referred to as *clipping functions*). Three examples of clipping functions are shown in Fig. 1. The goal of solving the inverse problem is to find the unknown quantity u from the given $L_1, \ldots, L_N$, $f_1, \ldots, f_N$, and available (often noisy) data s.

A wide variety of physical measurements in practical situations can be modeled by Eq. (1) in a unified way. A typical example is a restoration problem of a band-limited continuous-time signal from its discrete and clipped samples. Here, $L_1, \ldots, L_N$ represent sampling, i.e., pointwise evaluations, of signals, and $f_1, \ldots, f_N$ represent clipping effects caused by sensors, amplifiers, and analog-to-digital converters. There are several related works on signal reconstruction methods and theories using nonclipped samples [1]–[3], clipped but uniform samples [4]. Several reconstruction methods for clipped signals [5]–[9] can be applied also in cases of nonuniform samples. Moreover, Rencker et al. [9] provided a discussion on influence of observational noises before clipping effects. However, formulation in these methods has discontinuous sensitivity against the observational noises after clipping effects, and a signal reconstruction method considering noises after clipping effects remains to be established and investigated. In addition, Eq. (1) includes many other examples such as measurements of various physical fields, e.g., electric, magnetic, and acoustic fields. For example, in an acoustic field measurement using multiple (omnidirectional or directional) microphones [10], [11], the directivity and frequency response of the microphones can be modeled by $L_1, \ldots, L_N$. Note that $L_1, \ldots, L_N$ are not limited to pointwise evaluations of functions, as this example shows.

In general, this inverse problem is ill-posed, i.e., the forward problem is not bijective and/or not continuous. Therefore, the following types of optimization problem are often used for determining the most reasonable solution:

$$\underset{u \in \mathcal{U}}{\text{minimize}} \quad Q_s(u) := D_f(Lu, s) + \frac{\delta}{2}\|u\|_{\mathcal{U}}^2, \tag{2}$$

where $L : \mathcal{U} \to \mathbb{R}^N$ and $f : \mathbb{R}^N \to \mathcal{S}$ are simplified notations of $L_1, \ldots, L_N$ and $f_1, \ldots, f_N$, respectively, i.e., $f(Lu) = (f_1(L_1 u), \ldots, f_N(L_N u))$, $D_f : \mathbb{R}^N \times \mathcal{S} \to (-\infty, +\infty]$ is a loss function, $\delta \in (0, +\infty)$ is a regularization parameter, and $\|\cdot\|_{\mathcal{U}}$ is the norm induced by the inner product $\langle \cdot, \cdot \rangle_{\mathcal{U}}$ on $\mathcal{U}$. Here, $Q_s : \mathcal{U} \to (-\infty, +\infty]$ is an objective function for evaluating the reasonability of u under the given s, which is composed of two terms on the right-hand side of Eq. (2). The first term evaluates the consistency between Lu and s under f. On the other hand, the second term is added to avoid divergence of the solution and determined independently of the observation. The following regularized least squares is one of the most commonly used formulations in the form of Eq. (2):

$$\underset{u \in \mathcal{U}}{\text{minimize}} \quad Q_s(u) := \frac{1}{2}\|f(Lu) - s\|_{\mathbb{R}^N}^2 + \frac{\delta}{2}\|u\|_{\mathcal{U}}^2. \tag{3}$$

Manuscript received January 12, 2021.
Manuscript publicized February 25, 2021.

[†]The authors are with the University of Tokyo, Tokyo, 113-8656 Japan.
a) E-mail: natsuki.ueno@ieee.org

DOI: 10.1587/transfun.2021EAP1004

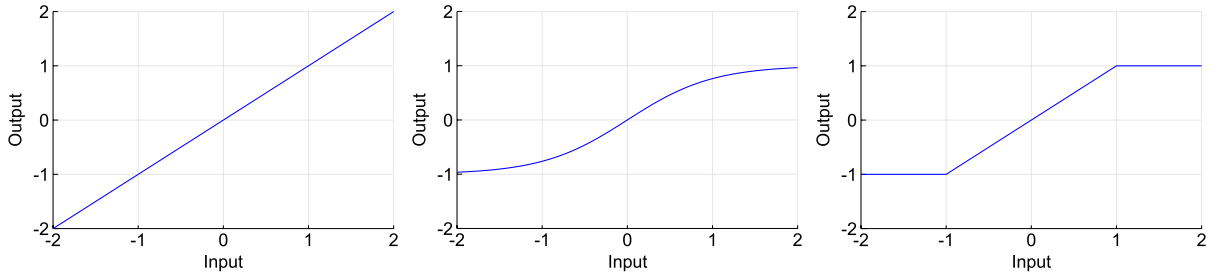

Fig. 1 Examples of clipping functions.

Various regularization methods have been proposed and analyzed in innumerable works (see, for example, [12]–[15] for an overview).

The optimization problem of Eq. (2) or (3) includes two difficulties. One is that $\mathcal{U}$ may have infinite dimensions. This problem can be overcome using the representer theorem [16]–[21], which states that the optimal solution of Eq. (2) can be represented as an N-linear combination of certain vectors determined by $L_1, \ldots, L_N$. Therefore, we need only to seek the optimal (finitely many) coefficients of these vectors. Although this theorem is typically applied to kernel methods [22], [23] in machine learning because of its affinity for reproducing kernel Hilbert spaces [24], [25], it is also useful in physical measurements. For example, the authors proposed an acoustic field estimation method based on the representer theorem for cases when f is linear [26]. When the observation includes nonlinear clipping effects, however, there still remains another difficulty even with the aid of the representer theorem; even a commonly used regularized least squares, i.e., Eq. (3), is not necessarily convex and differentiable with respect to the optimization variables owing to the nonlinearity or nondifferentiability of f. Therefore, an alternative formulation of the loss function that is easy to optimize is desired from a practical viewpoint.

In this paper, we propose a tractable formulation where the loss function is convex and differentiable with respect to the optimization variables and has a divergence-like property, i.e., it is minimized if and only if $s = f(Lu)$. By using our proposed formulation in combination with the representer theorem, we need only to deal with a finite-dimensional, convex, and differentiable optimization problem without any constraints, which can be solved easily by using well-established algorithms such as gradient descent, nonlinear conjugate gradient descent, and quasi-Newton methods [27]–[31]. This loss function is designed using the primitive functions of the clipping functions and also related closely to the concept of the Bregman divergence. Even in cases where another loss function such as Eq. (3) is considered to be suitable from a stochastic or other viewpoint, a good initial solution can be obtained by using our proposed formulation owing to its convexity. We also provide two practical examples, estimation problems of band-limited signals from their time-sampled values and time-harmonic acoustic fields using pressure-gradient microphones, and evaluate the validity of our theory by numerical experiments.

The rest of this paper is organized as follows. In Sect. 2, we introduce the representer theorem. In Sect. 3, we propose a convex and differentiable formulation of the loss function in Eq. (2). In Sect. 4, we show two practical examples of inverse problems in which our theory can be applied, and the results of their numerical experiments are provided. Finally, we present our conclusion in Sect. 5.

2. Representer Theorem

We introduce the representer theorem, which guarantees that Eq. (2) can be reduced to an optimization problem with respect to N variables. Since there are several related results [16]–[21], all of which are called representer theorems, we provide here a suitable form for Eq. (2) also with extension to local solutions [18]. This extension is essential because we also consider nonconvex formulation such as Eq. (3) with initialization using our proposed convex formulation. This theorem is effective, especially when $\mathcal{U}$ has infinite dimensions; however, it is also useful when $\mathcal{U}$ has finite but much larger dimensions than N because it may contribute to a significant reduction of computational cost in the optimization.

2.1 Preliminaries

First, we introduce the Riesz representation theorem for Hilbert spaces (see, e.g., [32], [33], for a proof).

Theorem 1: Let $(\mathcal{U}, \langle\cdot,\cdot\rangle_{\mathcal{U}})$ be a Hilbert space over $\mathbb{K}$ ($\mathbb{R}$ or $\mathbb{C}$) and $\Phi : \mathcal{U} \to \mathbb{K}$ be a bounded linear functional. Then, there exists a unique $\varphi \in \mathcal{U}$ satisfying

$$\Phi u = \langle \varphi, u \rangle_{\mathcal{U}} \quad \forall u \in \mathcal{U}. \tag{4}$$

From the Riesz representation theorem, for the bounded linear operator L defined in Sect. 1, there exists a unique sequence $(v_1, \ldots, v_N) \in \mathcal{U}^N$ satisfying

$$L_n u = \langle v_n, u \rangle_{\mathcal{U}} \quad \forall u \in \mathcal{U}, n \in \{1, \ldots, N\}. \tag{5}$$

Hereafter, we call v_n the *representation vector* of L_n and $(v_1, \ldots, v_N)$ the *representation vector sequence* of L.

Next, we define a Gram operator as follows.

Definition 2: Let $(\mathcal{U}, \langle\cdot,\cdot\rangle_{\mathcal{U}})$ be a Hilbert space over $\mathbb{K}$ ($\mathbb{R}$ or $\mathbb{C}$), N be a natural number, and $v_n \in \mathcal{U}$ be the representation vector of a bounded linear functional $L_n : \mathcal{U} \to \mathbb{K}$ for each $n \in \{1, \ldots, N\}$. Then, a linear mapping $K : \mathbb{K}^N \to \mathbb{K}^N$

whose representation matrix $\mathbf{K}$ is given as

$$\mathbf{K} \coloneqq \begin{bmatrix} K_{1,1} & \cdots & K_{1,N} \\ \vdots & \ddots & \vdots \\ K_{N,1} & \cdots & K_{N,N} \end{bmatrix} \tag{6}$$

with

$$K_{n_1,n_2} \coloneqq \langle v_{n_1}, v_{n_2} \rangle_{\mathcal{U}} = L_{n_1} v_{n_2} \quad \forall n_1, n_2 \in \{1, \ldots, N\} \tag{7}$$

is called a Gram operator generated by $(v_1 \ldots, v_N)$. This matrix $\mathbf{K}$ is always self-adjoint and positive-semidefinite, and it is positive-definite if and only if $(v_1, \ldots, v_N)$ is linearly independent. Furthermore, the semi-inner product and seminorm on $\mathbb{K}^N$ induced by K are denoted by $\langle \cdot, \cdot \rangle_K$ and $\| \cdot \|_K$, respectively, i.e.,

$$\langle \alpha, \beta \rangle_K \coloneqq \langle \alpha, K\beta \rangle_{\mathbb{K}^N} \quad \forall \alpha, \beta \in \mathbb{K}^N, \tag{8}$$

$$\|\alpha\|_K \coloneqq \sqrt{\langle \alpha, \alpha \rangle_K} \quad \forall \alpha \in \mathbb{K}^N. \tag{9}$$

2.2 Statement

In accordance with a prior work [17], we provide the statement for slightly more general conditions than those in Eq. (2); it can be easily confirmed that Eq. (2) satisfies these conditions. For an essential part of the proof, see [18].

Theorem 3: Assume the following conditions.

- $(\mathcal{U}, \langle \cdot, \cdot \rangle_{\mathcal{U}})$: Hilbert space over $\mathbb{K}$ ($\mathbb{R}$ or $\mathbb{C}$)
  - $\| \cdot \|_{\mathcal{U}}$: norm on $\mathcal{U}$ induced by the inner product $\langle \cdot, \cdot \rangle_{\mathcal{U}}$
- N : natural number
- $L : \mathcal{U} \to \mathbb{K}^N$ bounded linear operator
  - $(v_1, \ldots, v_N)$: representation vector sequence of L
  - K : Gram operator generated by $(v_1, \ldots, v_N)$
  - $\| \cdot \|_K$: seminorm on $\mathbb{K}^N$ induced by K
- $E : \mathbb{K}^N \to (-\infty, +\infty]$ arbitrary function
- $g : [0, +\infty) \to (-\infty, +\infty)$ strictly monotonically increasing function

Then, any global/local optimal point $u^{(\mathrm{opt})} \in \mathcal{U}$ of the optimization problem

$$\underset{u \in \mathcal{U}}{\text{minimize}} \quad Q(u) \coloneqq E(Lu) + g(\|u\|_{\mathcal{U}}) \tag{10}$$

admits the following representation:

$$u^{(\mathrm{opt})} = \sum_{n=1}^{N} \alpha_n^{(\mathrm{opt})} v_n. \tag{11}$$

Here, $\alpha^{(\mathrm{opt})} \coloneqq (\alpha_1^{(\mathrm{opt})}, \ldots, \alpha_N^{(\mathrm{opt})}) \in \mathbb{K}^N$ is given as a global/local optimal point of the optimization problem

$$\underset{\alpha \in \mathbb{K}^N}{\text{minimize}} \quad Q^{(*)}(\alpha) \coloneqq E(K\alpha) + g(\|\alpha\|_K). \tag{12}$$

More precisely, the following two propositions hold:

1. If and only if $u^{(\mathrm{opt})} \in \mathcal{U}$ is a global optimal point of Eq. (10), $u^{(\mathrm{opt})}$ can be represented in the form of $u^{(\mathrm{opt})} = \sum_{n=1}^{N} \alpha_n^{(\mathrm{opt})} v_n$ for some $\alpha^{(\mathrm{opt})} \coloneqq (\alpha_1^{(\mathrm{opt})}, \ldots, \alpha_N^{(\mathrm{opt})}) \in \mathbb{K}^N$ that is a global optimal point of Eq. (12).
2. If and only if $u^{(\mathrm{opt})} \in \mathcal{U}$ is a local optimal point of Eq. (10), $u^{(\mathrm{opt})}$ can be represented in the form of $u^{(\mathrm{opt})} = \sum_{n=1}^{N} \alpha_n^{(\mathrm{opt})} v_n$ for some $\alpha^{(\mathrm{opt})} \coloneqq (\alpha_1^{(\mathrm{opt})}, \ldots, \alpha_N^{(\mathrm{opt})}) \in \mathbb{K}^N$ that is a local optimal point of Eq. (12).

Remark 4: With respect to the term "local", we consider the standard topologies on $\mathcal{U}$ and $\mathbb{K}^N$ induced by the norms $\| \cdot \|_{\mathcal{U}}$ and $\| \cdot \|_{\mathbb{K}^N}$, respectively. In particular, $u^{(\mathrm{opt})} \in \mathcal{U}$ is called a local optimal point of Eq. (10) if and only if $Q(u^{(\mathrm{opt})}) < +\infty$ and there exists some $\epsilon \in (0, +\infty)$ satisfying $Q(u^{(\mathrm{opt})}) \leq Q(u)$ $\forall u \in \mathcal{B}(u^{(\mathrm{opt})}; \epsilon)$. Here, for $u_0 \in \mathcal{U}$ and $\epsilon \in (0, +\infty)$, $\mathcal{B}(u_0; \epsilon) \subset \mathcal{U}$ denotes the open ball centered at u_0 with radius ϵ, i.e., $\mathcal{B}(u_0; \epsilon) \coloneqq \{u \in \mathcal{U} \mid \|u - u_0\|_{\mathcal{U}} < \epsilon\}$.

3. Convex Formulation

In this section, we present a tractable formulation of the loss function D and provide a concrete discussion for solving the optimization problem by computation.

3.1 Formulation

Let $F_1, \ldots, F_N : \mathbb{R} \to \mathbb{R}$ denote primitive functions of $f_1, \ldots, f_N$, respectively. Note that $F_1, \ldots, F_N$ are differentiable and convex because $f_1, \ldots, f_N$ are continuous and monotonically increasing. In addition, the ranges of $f_1, \ldots, f_N$ are respectively denoted by $\mathcal{S}_1, \ldots, \mathcal{S}_N \subseteq \mathbb{R}$. Then, we define the loss function D_f as

$$D_f(z, s) \coloneqq \sum_{n=1}^{N} d_n(z_n, s_n)$$
$$\forall z \coloneqq (z_1, \ldots, z_N) \in \mathbb{R}^N, s \coloneqq (s_1, \ldots, s_N) \in \mathcal{S} \tag{13}$$

with

$$d_n(z_n, s_n) \coloneqq \frac{1}{\sigma_n^2}[F_n(z_n) - F_n(f_n^{-1}(s_n)) - s_n(z_n - f_n^{-1}(s_n))]$$
$$\forall z_n \in \mathbb{R}, s_n, \in \mathcal{S}_n, n \in \{1, \ldots, N\}, \tag{14}$$

where $\sigma_1, \ldots, \sigma_N \in (0, +\infty)$ are dispersion parameters representing the observational uncertainty. Although $f_1, \ldots, f_N$ is not uniquely invertible in general, this is a well-defined function because any choice of $f_n^{-1}(s_n)$ in Eq. (14) yields the same value (see Appendix A). This loss function has the following divergence-like properties.

1. $D_f(z, s) \geq 0$ $\forall z \in \mathbb{R}^N, s \in \mathcal{S}$.
2. $D_f(z, s) = 0$ if and only if $s = f(z)$.

Proofs of these properties are provided in Appendix B. In

cases of a strictly monotonically increasing f_n, d_n can also be represented as $d_n(z_n, s_n) = B_{F_n}(z_n, f_n^{-1}(s_n))/\sigma_n^2\ \forall z_n, \in \mathbb{R}, s_n \in \mathcal{S}_n$, where $B_{F_n} : \mathbb{R} \times \mathbb{R} \to [0, +\infty)$ denotes the Bregman divergence associated with F_n. Moreover, if f_n is the identity function, d_n is a weighted squared error function defined as $d_n(z_n, s_n) = (z_n - s_n)^2/(2\sigma_n^2)\ \forall z_n, s_n \in \mathbb{R}$. Using Eq. (14), we obtain the objective function as

$$Q_s(u) \coloneqq \sum_{n=1}^{N} \frac{1}{\sigma_n^2}[F_n(L_n u) - F_n(f_n^{-1}(s_n)) - s_n(L_n u_n - f_n^{-1}(s_n))] + \frac{\delta}{2}\|u\|_{\mathcal{U}}^2. \quad (15)$$

This can be simplified by omitting the terms irrelevant to the optimization variable as

$$Q_s(u) = \sum_{n=1}^{N} \frac{1}{\sigma_n^2}\left(F_n(L_n u) - s_n L_n u\right) + \frac{\delta}{2}\|u\|_{\mathcal{U}}^2 + C, \quad (16)$$

where $C \in \mathbb{R}$ is a constant.

From Theorem 3, the minimization problem of Eq. (16) on $\mathcal{U}$ can be recast to the minimization problem of the following objective function on $\mathbb{R}^N$:

$$Q_s^{(*)}(\alpha) \coloneqq \sum_{n=1}^{N} \frac{1}{\sigma_n^2}\left(F_n(K_n\alpha) - s_n K_n\alpha\right) + \frac{\delta}{2}\|\alpha\|_K^2 + C, \quad (17)$$

where $K_n : \mathbb{R}^N \to \mathbb{R}$ is a linear mapping whose representation matrix (a row vector) $\mathbf{K}_n$ is given by

$$\mathbf{K}_n \coloneqq [K_{n,1}, \ldots, K_{n,N}] \quad \forall n \in \{1, \ldots, N\}. \quad (18)$$

Then, $Q_s^{(*)}$ is a convex function because the functions $F_n(K_n\alpha)$, $-s_n K_n\alpha$, and $\|\alpha\|_K^2$ are convex with respect to α (all of the following functions are convex: linear functions, seminorm functions[†], composition of a convex function and linear transformation, square of a convex nonnegative function, and nonnegative weighted sums of convex functions [30]).

Note that Eq. (16) can be defined even when $s \notin \mathcal{S}$ (due to observational noises) by ignoring the constant C. Also in this case, the exsitence of the solution is guaranteed because Q_s (where C is omitted) is continuous and coercive (see Appendix C); therefore, one can use the proposed formulation regardless of whether or not s is in $\mathcal{S}$. It should be also noted that most related works [6]–[9] cannot be used in such cases.

3.2 Derivation of Gradient

As described above, the objective function $Q_s^{(*)}$ is convex and has no constraint. In addition, $Q_s^{(*)}$ is partially differentiable, and the gradient of $Q_s^{(*)}$ is given by

$$\frac{\partial}{\partial\alpha_i}Q_s^{(*)}(\alpha) = \sum_{n=1}^{N} \frac{1}{\sigma_n^2}(f_n(K_n\alpha) - s_n)K_{n,i} + \delta K_i\alpha \quad \forall i \in \{1, \ldots, N\}. \quad (19)$$

Therefore, many well-established iterative algorithms using the gradient of $Q_s^{(*)}$, such as gradient descent, nonlinear conjugate gradient descent, and quasi-Newton methods, are available for the minimization of $Q_s^{(*)}$.

Furthermore, if $f_1, \ldots, f_N$ are η-Lipschitz continuous with $\eta \in [0, +\infty)$, the gradient of $Q_s^{(*)}$ is also Lipschitz continuous with a Lipschitz constant $\eta M_K^2/\sigma_{\min}^2 + \delta M_K$, where M_K denotes the maximum eigenvalue of the representation matrix of K and $\sigma_{\min}$ denotes the minimum value of $\{\sigma_1, \ldots, \sigma_N\}$. In this case, the global convergence is guaranteed in many iterative algorithms including a gradient descent with a fixed step size [27] and an accelerated gradient descent [28].

4. Application Examples and Numerical Experiments

We provide two examples of inverse problems to which our proposed formulation can be applied. Hereafter, for any measurable set $\mathcal{X} \subseteq \mathbb{R}$ and measurable function $\rho : \mathcal{X} \to \mathbb{C}$ with respect to the Lebesgue measure, $\int_{x\in\mathcal{X}} \rho(x)\,\mathrm{d}\mu$ denotes the Lebesgue integral of ρ on $\mathcal{X}$.

4.1 Estimation of Band-Limited Signals

First, we provide an example of an estimation problem of band-limited signals from their irregularly time-sampled values with soft clipping effects.

4.1.1 Formulation

A band-limited signal can be modeled as a function $u : \mathbb{R} \to \mathbb{R}$ in the form of

$$u(t) = \frac{1}{\sqrt{2\pi}}\int_{\omega\in\Omega} \hat{u}(\omega)\exp(\mathrm{i}\omega t)\,\mathrm{d}\mu \quad \forall t \in \mathbb{R} \quad (20)$$

with a square-integrable function $\hat{u} : \Omega \to \mathbb{C}$, where $\Omega \coloneqq [-\omega_{\max}, \omega_{\max}]$ and $\omega_{\max} \in (0, +\infty)$ denotes the maximum angular frequency of target signals. Therefore, we define a real Hilbert space $\mathcal{U}$ and its inner product $\langle\cdot,\cdot\rangle_{\mathcal{U}}$ as

$$\mathcal{U} \coloneqq \left\{u : \mathbb{R} \to \mathbb{R} \;\middle|\; \exists\hat{u} : \Omega \to \mathbb{C} \text{ s.t. } \int_{\omega\in\Omega} |\hat{u}(\omega)|^2\,\mathrm{d}\mu < +\infty,\ u = \mathfrak{F}\hat{u}\right\}, \quad (21)$$

and

$$\langle u_1, u_2\rangle_{\mathcal{U}} \coloneqq \int_{t\in\mathbb{R}} u_1(t)u_2(t)\,\mathrm{d}\mu, \quad (22)$$

[†]In [30], the convexity of norm functions is shown; however, it can be extended immediately to seminorm functions because only the triangle inequality and absolute homogeneity are sufficient to yield its convexity.

respectively, where $\mathfrak{F}$ denotes the transform of functions defined as Eq. (20).

We consider the forward problem in the form of Eq. (1) with

$$L_n u \coloneqq u(\mathrm{t}_n) \quad \forall u \in \mathcal{U}, n \in \{1, \dots, N\}, \tag{23}$$

$$f_n(z) \coloneqq \tau \tanh(z/\tau) \quad \forall z \in \mathbb{R}, n \in \{1, \dots, N\}, \tag{24}$$

where $(\mathrm{t}_1, \dots, \mathrm{t}_N) \in \mathbb{R}^N$ are sampling times and $\tau \in (0, +\infty]$ represents a clipping level ($\tau = +\infty$ means that $f_1, \dots, f_N$ are the identical functions).

In this case, v_n and K_{n_1,n_2} are given by

$$v_n(t) = \frac{\omega_{\max}}{\pi} \mathrm{sinc}(\omega_{\max}(t - \mathrm{t}_n)) \quad \forall t \in \mathbb{R}, n \in \{1, \dots, N\}, \tag{25}$$

and

$$K_{n_1,n_2} = \frac{\omega_{\max}}{\pi} \mathrm{sinc}(\omega_{\max}(\mathrm{t}_{n_2} - \mathrm{t}_{n_1})) \quad \forall n_1, n_2 \in \{1, \dots, N\}, \tag{26}$$

respectively, where $\mathrm{sinc}(\cdot)$ is the unnormalized sinc function defined as $\mathrm{sinc}(0) \coloneqq 1$ and $\mathrm{sinc}(z) \coloneqq \sin(z)/z$ for $z \in \mathbb{R} \setminus \{0\}$. These are derived by the fact that the sinc function is the reproducing kernel of $\mathcal{U}$, as noted in [34], [35].

4.1.2 Experimental Evaluation

We conducted numerical experiments using Julia v.1.2.0 whose settings are given in Table 1. Here, noisy observation was simulated. Note that observation noise was added after the clipping effects (therefore, mere inversion of f causes significant amplification of the noise). We compared the following five conditions: clipped (**Proposed**, **SC**: soft consistency, **RLS**: regularized least squares, and **Proposed+RLS**) and nonclipped (**Proposed**). Under the clipped (**Proposed**, **RLS**, and **Proposed+RLS**) conditions, τ was set as 1. Under the nonclipped (**Proposed**) condition, on the other hand, τ was set as $+\infty$. Under the clipped (**Proposed**) and nonclipped (**Proposed**) conditions, the optimal solutions $u^{(\mathrm{opt})} \in \mathcal{U}$ were obtained by minimizing Eq. (17) with an initial value of zero. Under the clipped (**SC**) condition, the objective function was defined using the *soft consistency* loss function [9] as

$$Q_{\mathrm{SC},s}(u) \coloneqq \sum_{n=1}^{N} \frac{1}{2\sigma_n^2} (L_n u - \Pi_{C_n}(L_n u))^2 + \frac{\delta}{2} \|u\|_{\mathcal{U}}^2, \tag{27}$$

where $C_n \subseteq \mathbb{R}$ is the feasible set defined as $C_n \coloneqq \{z \in \mathbb{R} \mid f(z) = s_n\}$, and $\Pi_{C_n}(\cdot)$ denotes the orthogonal projection into C_n for each $n \in \{1, \dots, N\}$ (the Euclidean-distance-based loss function is used here although the method of [9] can be combined with other loss functions such as the Huber loss function). On the basis of Theorem 3, the optimal solutions were obtained by minimizing

Table 1 Settings in band-limited signal estimation.

$\omega_{\max}$	$\omega_{\max} \coloneqq 2\pi \mathrm{f}_{\max}$ with $\mathrm{f}_{\max} = 100\,\mathrm{Hz}$.
u	$u(t) \coloneqq \sum_{\nu=0}^{200} a_\nu \mathrm{sinc}(\omega_{\max} t - \nu\pi)$.
$(a_0, \dots, a_{200})$	Sampled independently from the univariate real normal distribution with mean 0 and variance 1.
N	$N \coloneqq 500$.
$(t_1, \dots, t_N)$	Sampled independently from the uniform distribution on $[0, 1]$ s.
τ	$\tau \coloneqq 1$ (clipped), $\tau \coloneqq +\infty$ (nonclipped).
Observation noise	Added to each $f_n(L_n u)$ for $n \in \{1, \dots, N\}$ independently from the univariate real normal distribution with mean 0 and variance $10^{-3} \times \|f(Lu)\|_{\mathbb{R}^N}^2 / N$.
δ, $(\sigma_1^2, \dots, \sigma_N^2)$	$\delta \coloneqq 10^{-1.5}$, $\sigma_n^2 \coloneqq 1$ $\forall n \in \{1, \dots, N\}$.
Evaluation criterion	$\mathrm{NMSE} \coloneqq 10 \log_{10}(\mathrm{E}/\mathrm{S})$, where $\mathrm{E} \coloneqq \sum_{i=1}^{N_t} \lvert u^{(\mathrm{opt})}(\mathrm{t}_i^{(\mathrm{eval})}) - u(\mathrm{t}_i^{(\mathrm{eval})})\rvert^2$, $\mathrm{S} \coloneqq \sum_{i=1}^{N_t} \lvert u(\mathrm{t}_i^{(\mathrm{eval})})\rvert^2$.
$(\mathrm{t}_1^{(\mathrm{eval})}, \dots, \mathrm{t}_{N_t}^{(\mathrm{eval})})$	Equally spaced points from 0 s to 1 s with intervals of 0.001 s ($N_t = 1001$).

$$Q_{\mathrm{SC},s}^{(*)}(\alpha) \coloneqq \sum_{n=1}^{N} \frac{1}{2\sigma_n^2} (K_n \alpha - \Pi_{C_n}(K_n \alpha))^2 + \frac{\delta}{2} \|\alpha\|_K^2 \tag{28}$$

with an initial value of zero. Here, for each $n \in \{1, \dots, N\}$, the signal s_n was discarded when it was outside the range of f_n owing to the observational noise since C_n cannot be defined for such s_n. Under the clipped (**RLS**) condition, the objective function was defined as the following regularized least squares:

$$Q_{\mathrm{LSQ},s}(u) \coloneqq \sum_{n=1}^{N} \frac{1}{2\sigma_n^2} (f_n(L_n u) - s_n)^2 + \frac{\delta}{2} \|u\|_{\mathcal{U}}^2. \tag{29}$$

On the basis of Theorem 3, the optimal solutions were obtained by minimizing

$$Q_{\mathrm{LSQ},s}^{(*)}(\alpha) \coloneqq \sum_{n=1}^{N} \frac{1}{2\sigma_n^2} (f_n(K_n \alpha) - s_n)^2 + \frac{\delta}{2} \|\alpha\|_K^2 \tag{30}$$

with an initial value of zero. Under the clipped (**Proposed+RLS**) condition, Eq. (17) was minimized first with an initial value of zero, and then Eq. (30) was minimized using the obtained solution of Eq. (17) as the initial value. In the optimization, we used a nonlinear conjugate gradient in Optim.jl [36] with the default settings. We evaluated the estimation performance by using the normalized mean squared error (NMSE). The results are provided in Table 2. Since some parameters were randomly determined, the mean and standard deviation of the NMSEs over 50 trials were calculated. We also plotted the true and estimated

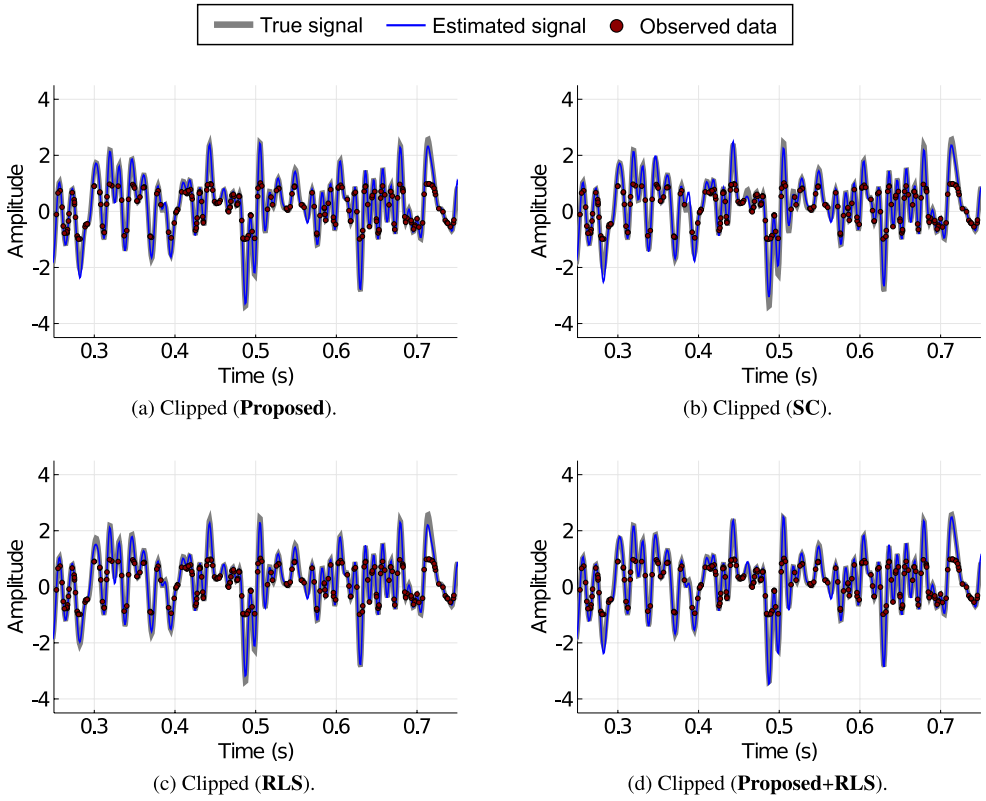

(a) Clipped (**Proposed**). (b) Clipped (**SC**).

(c) Clipped (**RLS**). (d) Clipped (**Proposed+RLS**).

Fig. 2 Results of band-limited signal estimation in [0.25, 0.75] s in the first trial. The NMSEs were (a) −23.33, (b) −18.28, (c) −20.89, and (d) −24.20 dB.

Table 2 Results of band-limited signal estimation (50 trials).

Condition	NMSE: mean ± standard deviation
Clipped (**Proposed**)	−19.67 ± 3.64 dB
Clipped (**SC**)	−15.94 ± 3.87 dB
Clipped (**RLS**)	−16.84 ± 2.19 dB
Clipped (**Proposed+RLS**)	−21.70 ± 3.25 dB
Nonclipped (**Proposed**)	−25.66 ± 3.70 dB

signals in the first trial in Fig. 2. The estimation accuracy for clipped (**SC**) was lowest, which means its lack of robustness against observational noises after clipping effects. Also the estimation accuracy for clipped (**RLS**) was low, which was considered to be due to its nonconvexity. On the other hand, the estimation accuracy for clipped (**Proposed**) was higher than that for clipped (**RLS**), and it was further improved by clipped (**Proposed+RLS**), which was close to that for nonclipped (**Proposed**). One possible reason why clipped (**Proposed+RLS**) outperformed clipped (**Proposed**) is because the formulation of **RLS** is well suited for Gaussian noises; it can be interpreted formally as a maximum a posteriori (MAP) estimation when the observational noises follow Gaussian distributions. From these results, one can see that an accurate estimation was achieved using the formulation of Eq. (17), which could also be used as an initial value in the optimization of a different formulation.

4.2 Estimation of Time-Harmonic Acoustic Fields

Next, we provide an example of an estimation problem of time-harmonic acoustic fields using pressure-gradient microphones (also called velocity microphones) with hard clipping effects.

4.2.1 Formulation

Consider the following two-dimensional acoustic wave equation:

$$\left(\frac{\partial^2}{\partial x^2} + \frac{\partial^2}{\partial y^2} - \frac{1}{\mathrm{c}^2}\frac{\partial^2}{\partial t^2}\right) u(x, y, t) = 0 \quad \forall x, y, t \in \mathbb{R}. \tag{31}$$

Here, $u(x, y, t) \in \mathbb{R}$ denotes the sound pressure at a position $(x, y) \in \mathbb{R}^2$ and a time $t \in \mathbb{R}$, and $\mathrm{c} \in (0, +\infty)$ denotes the speed of sound. One of the solutions for Eq. (31) is a complex sinusoidal plane wave function defined as

$$\varphi(x, y, t; \theta) \coloneqq \exp\left(\mathrm{i}\omega_0\left(t - \frac{x\cos\theta + y\sin\theta}{\mathrm{c}}\right)\right) \quad \forall x, y, t \in \mathbb{R}, \tag{32}$$

where $\omega_0 \in (0, +\infty)$ denotes an angular frequency and $\theta \in [0, 2\pi)$ denotes a polar angle of the traveling direction of the

plane wave. As a superposition of plane waves, the time-harmonic incident acoustic field with angular frequency ω_0 can be well modeled as

$$u(x, y, t) = \int_{\theta\in[0,2\pi)} \mathrm{Re}\left(\mathring{u}(\theta)\varphi(x, y, t; \theta)\right) \mathrm{d}\mu \quad \forall x, y, t \in \mathbb{R} \tag{33}$$

with a square-integrable function $\mathring{u} : [0, 2\pi) \to \mathbb{C}$. We define a real Hilbert space $\mathcal{U}$ and its inner product $\langle\cdot,\cdot\rangle_{\mathcal{U}}$ as

$$\mathcal{U} := \left\{ u : \mathbb{R}^3 \to \mathbb{R} \;\middle|\; \exists \mathring{u} : [0, 2\pi) \to \mathbb{C} \text{ s.t. } \int_{\theta\in[0,2\pi)} |\mathring{u}(\theta)|^2 \,\mathrm{d}\mu < +\infty,\ u = \mathfrak{H}\mathring{u} \right\} \tag{34}$$

and

$$\langle u_1, u_2\rangle_{\mathcal{U}} := \int_{\theta\in[0,2\pi)} \mathrm{Re}\left(\mathring{u}_1(\theta)^* \mathring{u}_2(\theta)\right) \mathrm{d}\mu, \tag{35}$$

respectively, where $\mathfrak{H}$ denotes the transform of functions defined as Eq. (33) and $\mathring{u}_1, \mathring{u}_2 : [0, 2\pi) \to \mathbb{C}$ is functions satisfying $u_1 = \mathfrak{H}\mathring{u}_1$ and $u_2 = \mathfrak{H}\mathring{u}_2$.

Suppose M pressure-gradient microphones are located at $(\mathrm{x}_1, \mathrm{y}_1), \ldots, (\mathrm{x}_M, \mathrm{y}_M) \in \mathbb{R}^2$, and let $\mathrm{t}_1, \ldots, \mathrm{t}_{P_m} \in \mathbb{R}$ with a natural number P_m be the sampling times of the mth microphone for each $m \in \{1, \ldots, M\}$. We consider the forward problem in the form of Eq. (1) with

$$L_n u := A_m \frac{\partial}{\partial d(\theta_m)} u(\mathrm{x}_m, \mathrm{y}_m, \mathrm{t}_p) \quad \forall n := (m, p) \in \{(1, 1), \ldots, (M, P_M)\}, \tag{36}$$

$$f_n(z) := \begin{cases} -\tau & z \le -\tau \\ z & -\tau < z < \tau \\ \tau & z \ge \tau \end{cases} \quad \forall n := (m, p) \in \{(1, 1), \ldots, (M, P_M)\}. \tag{37}$$

Here, $A_m \in \mathbb{R}$ is a gain of the mth microphone, $\partial/\partial d(\theta_m)$ denotes the directional derivative along the direction $d(\theta_m) := (\cos\theta_m, \sin\theta_m)$ defined as

$$\frac{\partial}{\partial d(\theta_m)} u(\mathrm{x}_m, \mathrm{y}_m, \mathrm{t}_p) := \left(\cos\theta_m \frac{\partial}{\partial x} + \sin\theta_m \frac{\partial}{\partial y}\right) u(\mathrm{x}_m, \mathrm{y}_m, \mathrm{t}_p), \tag{38}$$

and $\tau \in (0, +\infty]$ is a clipping level. Note that $f_1, \ldots, f_N$ are noninvertible functions for $\tau \ne +\infty$. In this case, v_n and K_{n_1,n_2} are given respectively by

$$v_n(x, y, t) := 2\pi A_m \frac{\omega_0}{\mathrm{c}} J_1\left(\frac{\omega_0}{\mathrm{c}}\sqrt{(x - \mathrm{x}_m)^2 + (y - \mathrm{y}_m)^2}\right) \cdot \cos(\angle(x - \mathrm{x}_m, y - \mathrm{y}_m) - \theta_m)\cos(\omega_0(t - \mathrm{t}_p)) \quad \forall x, y, t \in \mathbb{R}, n := (m, p) \in \{(1, 1), \ldots, (M, P_M)\} \tag{39}$$

Table 3 Settings in time-harmonic acoustic field estimation.

ω_0	$\omega_0 := 2\pi\mathrm{f}_0$ with $\mathrm{f}_0 = 100\,\mathrm{Hz}$.
c	$\mathrm{c} = 340\,\mathrm{m/s}$.
u	$u(x, y, t) := \sum_{\nu=-10}^{10} \mathrm{Re}\left(a_\nu J_\nu\left(\frac{\omega_0}{\mathrm{c}}\sqrt{x^2 + y^2}\right) \cdot \exp(\mathrm{i}\nu\angle(x, y))\exp(\mathrm{i}\omega_0 t)\right)$.
$(a_{-10}, \ldots, a_{10})$	Sampled independently from the univariate circular-symmetric complex normal distribution with mean 0 and variance 1.
M, $(P_1, \ldots, P_M)$	$M := 12$, $P_m := 10\ \forall m \in \{1, \ldots, M\}$ $(N = 120)$.
$(\mathrm{x}_1, \ldots, \mathrm{x}_M)$, $(\mathrm{y}_1, \ldots, \mathrm{y}_M)$	Sampled independently from the uniform distribution on $[-2, 2]$ m.
$(\theta_1, \ldots, \theta_M)$	Sampled independently from the uniform distribution on $[0, 2\pi)$.
$(A_1, \ldots, A_M)$	$A_m = \mathrm{c}/\omega_0\ \forall m \in \{1, \ldots, M\}$.
$(\mathrm{t}_{(1,1)}, \ldots, \mathrm{t}_{(M,P_M)})$	Sampled independently from the uniform distribution on $[0, 0.01]$ s.
τ	$\tau = 0.5$ (clipped), $\tau = +\infty$ (nonclipped).
Observation noise	Added to each $f_n(L_n u)$ for $n \in \{(1, 1), \ldots, (M, P_M)\}$ independently from the univariate real normal distribution with mean 0 and variance $10^{-3} \times \|f(Lu)\|^2_{\mathbb{R}^N}/N$.
δ, σ_n^2	$\delta := 10^{-1.5}$, $\sigma_n^2 := 1$ $\forall n \in \{(1, 1), \ldots, (M, P_M)\}$.
Evaluation criterion	NMSE $:= 10\log_{10}(\mathrm{E}/\mathrm{S})$, where $\mathrm{E} := \sum_{i=1}^{N_x}\sum_{j=1}^{N_y}\sum_{k=1}^{N_t} \lvert u^{(\mathrm{opt})}(\mathrm{x}_i^{(\mathrm{eval})}, \mathrm{y}_j^{(\mathrm{eval})}, \mathrm{t}_k^{(\mathrm{eval})}) - u(\mathrm{x}_i^{(\mathrm{eval})}, \mathrm{y}_j^{(\mathrm{eval})}, \mathrm{t}_k^{(\mathrm{eval})})\rvert^2$, $\mathrm{S} := \sum_{i=1}^{N_x}\sum_{j=1}^{N_y}\sum_{k=1}^{N_t} \lvert u(\mathrm{x}_i^{(\mathrm{eval})}, \mathrm{y}_j^{(\mathrm{eval})}, \mathrm{t}_k^{(\mathrm{eval})})\rvert^2$.
$(\mathrm{x}_1^{(\mathrm{eval})}, \ldots, \mathrm{x}_{N_x}^{(\mathrm{eval})})$, $(\mathrm{y}_1^{(\mathrm{eval})}, \ldots, \mathrm{y}_{N_y}^{(\mathrm{eval})})$	Equally spaced points from -2 m to 2 m with intervals of 0.05 m ($N_x = 81$, $N_y = 81$).
$(\mathrm{t}_1^{(\mathrm{eval})}, \ldots, \mathrm{t}_{N_t}^{(\mathrm{eval})})$	Equally spaced points from 0 s to 0.01 s with intervals of 0.001 s ($N_t = 11$).

and

$$K_{n_1,n_2} := -\pi\left(A_m\frac{\omega_0}{\mathrm{c}}\right)^2 \left[J_2\left(\frac{\omega_0}{\mathrm{c}}\mathrm{r}_{m_2,m_1}\right) \cdot \cos(2\phi_{m_2,m_1} - \theta_{m_1} - \theta_{m_2}) - J_0\left(\frac{\omega_0}{\mathrm{c}}\mathrm{r}_{m_2,m_1}\right)\cos(\theta_{m_2} - \theta_{m_1})\right] \cdot \cos(\omega_0(\mathrm{t}_{p_2} - \mathrm{t}_{p_1})) \quad \forall n_1 := (m_1, p_1), n_2 := (m_2, p_2) \in \{(1, 1), \ldots, (M, P_M)\} \tag{40}$$

with

$$\mathrm{r}_{m_2,m_1} := \sqrt{(\mathrm{x}_{m_2} - \mathrm{x}_{m_1})^2 + (\mathrm{y}_{m_2} - \mathrm{y}_{m_1})^2} \tag{41}$$

$$\phi_{m_2,m_1} := \angle(\mathrm{x}_{m_2} - \mathrm{x}_{m_1}, \mathrm{y}_{m_2} - \mathrm{y}_{m_1}) \tag{42}$$

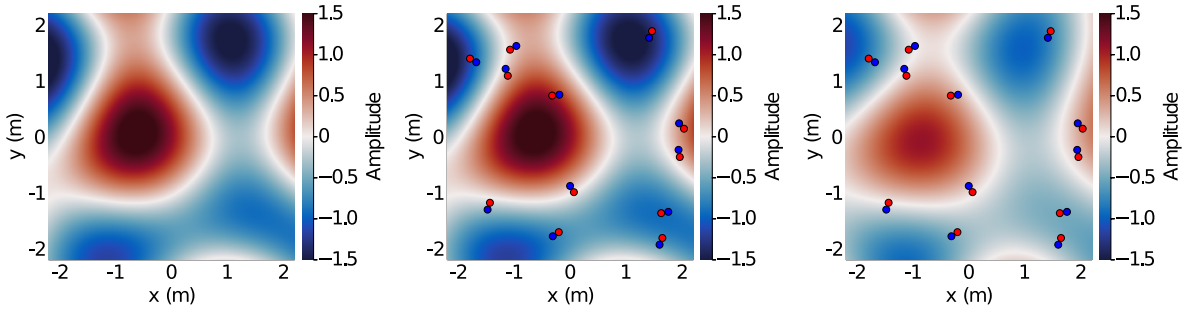

(a) True field. (b) Clipped (**Proposed**). (c) Clipped (**SC**).

Fig. 3 Results of time-harmonic acoustic field estimation at $t = 0$ s in the first trial. The NMSEs were (b) −17.83 and (c) −6.82 dB. The clipping distortion was −8.07 dB.

Table 4 Results of time-harmonic acoustic field estimation (50 trials).

Condition	NMSE: mean ± standard deviation
Clipped (**Proposed**)	−12.33 ± 5.01 dB
Clipped (**SC**)	−6.97 ± 3.65 dB
Nonclipped (**Proposed**)	−17.25 ± 4.30 dB

Here, $J_\nu(\cdot)$ denotes the νth-order Bessel function of the first kind for each integer ν and $\angle(x, y)$ denotes the polar angle of (x, y) for each $x, y \in \mathbb{R}$. The derivations of v_n and K_{n_1,n_2} are given in detail in Appendix D.

4.2.2 Experimental Evaluation

We conducted numerical experiments using Julia v.1.2.0 whose settings are given in Table 3. Among the five conditions investigated in Sect. 4.1.2, clipped (**Proposed** and **SC**) with $\tau = 0.5$ and nonclipped (**Proposed**) with $\tau = +\infty$ were compared in this experiment because Eq. (30) is not differentiable with respect to the optimization variables. Here, under the clipped (**SC**) condition, each of s_n for $n \in \{1, \ldots, N\}$ was projected into $\mathcal{S}_n$, i.e., $[-\tau, \tau]$, as a preprocessing (note that this preprocessing was unavailable in the experiments in Sect. 4.1.2 since $\mathcal{S}_n$ is an open set in that case). The results from 50 trials are shown in Table 4. The clipping distortion defined as $10 \log_{10} \|f(Lu) - Lu\|^2_{\mathbb{R}^N} / \|Lu\|^2_{\mathbb{R}^N}$ was also calculated, and its mean ± standard deviation for 50 trials was -10.18 ± 3.87 dB. In addition, we show the true and estimated acoustic fields in the first trial in Fig. 3. Here, pairs of red and blue circles represent the position and orientation of the pressure-gradient microphones; the direction from the blue circle to the red circle corresponds to the direction of the derivative that the pressure-gradient microphone observed. Even under the hard clipping effects, clipped (**Proposed**) achieved an estimation performance relatively close to that of nonclipped (**Proposed**), compared with the value of the clipping distortion. We can also see that clipped (**Proposed**) outperformed clipped (**SC**), as was the case in the experiments in Sect. 4.1.2.

5. Conclusion

We presented a new useful formulation for ill-posed inverse problems in Hilbert spaces with nonlinear clipping effects. A loss function was designed so that it was convex and differentiable with respect to the optimization variables. By using this formulation in combination with the representer theorem, we derived a tractable optimization problem that is easy to optimize using well-established algorithms. Finally, we provided two practical examples of inverse problems with soft and hard clipping effects, and the experimental evaluations confirmed the validity of our proposed formulation.

Acknowledgments

This work was supported by JSPS KAKENHI Grant Number JP18J21926, JST PRESTO Grant Number JPMJPR18J4, and SECOM Science and Technology Foundation.

References

[1] M. Unser, "Sampling — 50 years after Shannon," Proc. IEEE, vol.88, no.4, pp.569–587, 2000.
[2] R. Tao, B.Z. Li, Y. Wang, and G.K. Aggrey, "On sampling of band-limited signals associated with the linear canonical transform," IEEE Trans. Signal Process., vol.56, no.11, pp.5454–5464, 2008.
[3] A. Tanaka, H. Imai, and M. Miyakoshi, "Kernel-induced sampling theorem," IEEE Trans. Signal Process., vol.58, no.7, pp.3569–3577, 2010.
[4] S.J. Godsill, P.J. Wolfe, and W.N.M. Fong, "Statistical model-based approaches to audio restoration and analysis," J. New Music Res., vol.30, no.4, pp.323–338, 2001.
[5] B. Defraene, N. Mansour, S.D. Hertogh, T. van Waterschoot, M. Diehl, and M. Moonen, "Declipping of audio signals using perceptual compressed sensing," IEEE Trans. Audio, Speech, Language Process., vol.21, no.12, pp.2627–2637, 2013.
[6] S. Kitić, N. Bertin, and R. Gribonval, "Sparsity and cosparsity for audio declipping: A flexible non-convex approach," Proc. 12th International Conference on Latent Variable Analysis and Signal Separation, pp.243–250, 2015.
[7] S. Kitić, L. Jacques, N. Madhu, M.P. Hopwood, A. Spriet, and C.D. Vleeschouwer, "Consistent iterative hard thresholding for signal declipping," Proc. IEEE International Conference on Acoustics, Speech, and Signal Processing, Vancouver, pp.5939–5943, May 2013.

[8] L. Rencker, F. Bach, W. Wang, and M.D. Plumbley, "Fast iterative shrinkage for signal declipping and dequantization," Proc. iTWIST'18, Marseille, paper-ID: 4, Nov. 2018.
[9] L. Rencker, F. Bach, W. Wang, and M.D. Plumbley, "Sparse recovery and dictionary learning from nonlinear compressive measurements," IEEE Trans. Signal Process., vol.67, no.21, pp.5659–5670, 2019.
[10] M.A. Poletti, "Three-dimensional surround sound systems based on spherical harmonics," J. Audio Engineering Society, vol.53, no.11, pp.1004–1025, 2005.
[11] N. Ueno, "Sound field recording using distributed microphones based on harmonic analysis of infinite order," IEEE Signal Process. Lett., vol.25, no.1, pp.135–139, 2017.
[12] H.W. Engl, M. Hanke, and A. Neubauer, Regularization of Inverse Problems, Kluwer Academic Publishers, Dordrecht, 1996.
[13] C.R. Vogel, Computational Methods for Inverse Problems, SIAM, Philadelphia, 2002.
[14] A. Kirsch, An Introduction to the Mathematical Theory of Inverse Problems, Springer Science & Business Media, New York, 2011.
[15] M. Benning and M. Burger, "Modern regularization methods for inverse problems," Acta Numerica, vol.27, no.1, pp.1–111, 2018.
[16] G. Wahba, Spline Models for Observational Data, SIAM, Philadelphia, 1990.
[17] B. Schölkopf, R. Herbrich, and A.J. Smola, "A generalized representer theorem," Proc. Computational Learning Theory, pp.416–426, 2001.
[18] C.A. Micchelli and M. Pontil, "Kernels for multi-task learning," Advances in Neural Information Processing Systems 17, pp.921–928, 2004.
[19] F. Dinuzzo and B. Schölkopf, "The representer theorem for Hilbert spaces: A necessary and sufficient condition," Advances in Neural Information Processing Systems 25, pp.189–196, 2012.
[20] R. Wang and Y. Xu, "Functional reproducing kernel Hilbert spaces for non-point-evaluation functional data," Appl. Comput. Harmon. Anal., vol.46, no.3, pp.569–623, 2019.
[21] M. Unser, "A unifying representer theorem for inverse problems and machine learning," arXiv:1903.00687, 2019.
[22] T. Hofmann, B. Schölkopf, and A.J. Smola, "Kernel methods in machine learning," Ann. Statist., vol.36, no.3, pp.1171–1220, 2008.
[23] K.P. Murphy, Machine Learning: A Probabilistic Perspective, MIT Press, Cambridge, 2012.
[24] N. Aronszajn, "Theory of reproducing kernels," Trans. Ame. Math. Soc., vol.68, no.3, pp.337–404, 1950.
[25] R.A. Kennedy and P. Sadeghi, Hilbert Space Methods in Signal Processing, Cambridge University Press, Cambridge, 2013.
[26] N. Ueno, S. Koyama, and H. Saruwatari, "Kernel ridge regression with constraint of Helmholtz equation for sound field interpolation," Proc. International Workshop on Acoustic Signal Enhancement, pp.436–440, 2018.
[27] L. Armijo, "Minimization of functions having Lipschitz continuous first partial derivatives," Pacific J. Math., vol.16, no.1, pp.1–3, 1966.
[28] Y.E. Nesterov, "A method of solving a convex programming problem with convergence rate $O(1/k^2)$," Doklady Akademii Nauk SSSR, vol.269, no.3, pp.543–547, 1983.
[29] C.T. Kelley, Iterative Methods for Linear and Nonlinear Equations, SIAM, Philadelphia, 1995.
[30] S. Boyd and L. Vandenberghe, Convex Optimization, Cambridge University Press, Cambridge, 2004.
[31] W.W. Hager and H. Zhang, "A survey of nonlinear conjugate gradient methods," Pacific J. Optimization, vol.2, no.1, pp.35–58, 2006.
[32] F. Riesz and B. Sz.-Nagy, Functional Analysis, Frederick Ungar Publishing, New York, 1955.
[33] J.B. Conway, A Course in Functional Analysis, Springer, New York, 2007.
[34] K. Yao, "Applications of reproducing kernel Hilbert spaces–bandlimited signal models," Information and Control, vol.11, no.4, pp.429–444, 1967.
[35] M.Z. Nashed and G.G. Walter, "General sampling theorems for functions in reproducing kernel Hilbert spaces," Math. Control, Signals, and Systems, vol.4, pp.363–390, 1991.
[36] P.K. Mogensen and A.N. Riseth, "Optim: A mathematical optimization package for Julia," J. Open Source Software, vol.3, no.24, p.615, 2018.
[37] G.N. Watson, A Treatise on the Theory of Bessel Functions, Cambridge University Press, Cambridge, 1995.

Appendix A: Well-Definedness of Loss Function

Assume $f_n(y_n) = f_n(w_n) = s_n$ and $y_n \le w_n$, and then we will prove

$$F_n(y_n) - s_n y_n = F_n(w_n) - s_n w_n, \tag{A·1}$$

which immediately yields the independence of $f_n^{-1}(s_n)$ in (14). First, since f_n is monotonically increasing and $f_n(y_n) = f_n(w_n)$, f_n takes a constant value s_n on the interval $[y_n, w_n]$. Therefore, we obtain

$$F_n(w_n) - F_n(y_n) = s_n(w_n - y_n), \tag{A·2}$$

which yields (A·1).

Appendix B: Properties of Loss Function

We show the following properties on d_n for each $n \in \{1, \dots, N\}$. Here, again note that $\tilde{z}_n = f_n^{-1}(s_n)$ and f_n is the derivative of F_n.

1. $d_n(z_n, s_n) \ge 0 \ \forall z_n \in \mathbb{R}, s_n \in \mathcal{S}_n$.
(Proof) It can be proved immediately from the following inequality on differentiable convex functions [30]:

$$F_n(z_n) - F_n(\tilde{z}_n) \ge f_n(\tilde{z}_n)(z_n - \tilde{z}_n) \quad \forall z_n, \tilde{z}_n \in \mathbb{R} \tag{A·3}$$

2. $d_n(z_n, s_n) = 0$ if and only if $s_n = f_n(z_n)$.
(Proof) In Eq. (A·3), the equality holds if and only if $f_n(z_n) = f_n(\tilde{z}_n)$. Therefore, we obtain

$$\begin{aligned} d_n(z_n, s_n) = 0 &\Leftrightarrow F_n(z_n) - F_n(f_n^{-1}(s_n)) \\ &\quad = s_n(z_n - f_n^{-1}(s_n)) \\ &\Leftrightarrow f_n(z_n) = f_n(f_n^{-1}(s_n)) \\ &\Leftrightarrow f_n(z_n) = s_n \end{aligned} \tag{A·4}$$

The above properties immediately yield the properties of D_f provided in Sect. 3.1.

Appendix C: Coerciveness of Proposed Formulation

We define $J : \mathbb{R} \to \mathbb{R}$ as

$$J(t) \coloneqq \sum_{n=1}^{N} \frac{1}{\sigma_n^2}(F_n(L_n(tu_0)) - s_n L_n(tu_0)) + \frac{\delta}{2}\|tu_0\|_{\mathcal{U}}^2 \tag{A·5}$$

for arbitrary fixed $u_0 \in \mathcal{U} \setminus \{0\}$, and then we will prove that

J is coercive, i.e., $\lim_{t\to-\infty} J(t) = +\infty$ and $\lim_{t\to+\infty} J(t) = +\infty$. First, the derivative of J, denoted by J', is given by

$$J'(t) = \sum_{n=1}^{N} \frac{1}{\sigma_n^2}(f_n(tL_nu_0) - s_n)L_nu_0 + t\delta\|u_0\|_{\mathcal{U}}^2. \tag{A·6}$$

Since $f_n(tL_nu_0)L_nu_0$ is monotonically increasing with respect to t for each $n \in \{1,\dots,N\}$, J' is also monotonically increasing, and moreover we obtain

$$\lim_{t\to-\infty} J'(t) = -\infty, \tag{A·7}$$

$$\lim_{t\to+\infty} J'(t) = +\infty. \tag{A·8}$$

Therefore, we obtain the coerciveness of J and also Q_s (where the constant C is omitted).

Appendix D: Derivation of Representation Vector Sequence and Gram Operator

Let $u \in \mathcal{U}$ be represented as Eq. (33) with a square-integrable function $\mathring{u} : [0, 2\pi) \to \mathbb{C}$ and φ_{θ_m} be defined as

$$\varphi_{\theta_m}(x, y, t; \theta) \coloneqq \frac{\partial}{\partial d(\theta_m)}\varphi(x, y, t; \theta) \quad \forall x, y, t \in \mathbb{R}, m \in \{1, \dots, M\}. \tag{A·9}$$

Then, by interchanging the integral and partial derivative (their interchangeability is proved later), we obtain

$$\frac{\partial}{\partial d(\theta_m)}u(x, y, t) = \int_{\theta\in[0,2\pi)} \mathrm{Re}(\mathring{u}(\theta)\varphi_{\theta_m}(x, y, t; \theta))\,\mathrm{d}\mu \quad \forall x, y, t \in \mathbb{R}, m \in \{1, \dots, M\}. \tag{A·10}$$

Here, for each $n \coloneqq (m, p) \in \{(1,1),\dots,(M, P_M)\}$, let $\mathring{v}_n$ and v_n be respectively defined as

$$\mathring{v}_n(\theta) \coloneqq A_m\varphi_{\theta_m}(\mathrm{x}_m, \mathrm{y}_m, \mathrm{t}_p; \theta)^* \quad \forall\theta \in [0, 2\pi), \tag{A·11}$$

$$v_n = \mathfrak{H}\mathring{v}_n, \tag{A·12}$$

which immediately yield

$$\begin{aligned}\langle v_n, u\rangle_{\mathcal{U}} &= A_m \int_{\theta\in[0,2\pi)} \mathrm{Re}\left(\mathring{u}(\theta)\varphi_{\theta_m}(\mathrm{x}_m, \mathrm{y}_m, \mathrm{t}_p; \theta)\right)\mathrm{d}\mu \\ &= L_nu.\end{aligned} \tag{A·13}$$

Therefore, v_n and K_{n_1,n_2} can be obtained as

$$\begin{aligned}&v_n(x, y, t) \\ &= A_m \int_{\theta\in[0,2\pi)} \mathrm{Re}\left(\varphi_{\theta_m}(\mathrm{x}_m, \mathrm{y}_m, \mathrm{t}_p; \theta)^*\varphi(x, y, t; \theta)\right)\mathrm{d}\mu \\ &= 2\pi A_m\frac{\omega_0}{\mathrm{c}}J_1\left(\frac{\omega_0}{\mathrm{c}}\sqrt{(x-\mathrm{x}_m)^2 + (y-\mathrm{y}_m)^2}\right) \\ &\quad\cdot\cos(\angle(x-\mathrm{x}_m, y-\mathrm{y}_m) - \theta_m)\cos(\omega_0(t-\mathrm{t}_p)) \\ &\quad \forall x, y, t \in \mathbb{R}, n \coloneqq (m, p) \in \{(1,1),\dots,(M, P_M)\}\end{aligned} \tag{A·14}$$

and

$$\begin{aligned}K_{n_1,n_2} &= A_m^2 \int_{\theta\in[0,2\pi)} \mathrm{Re}\Big(\varphi_{\theta_{m_2}}(\mathrm{x}_{m_2}, \mathrm{y}_{m_2}, \mathrm{t}_{p_2}; \theta)^* \\ &\qquad\cdot\varphi_{\theta_{m_1}}(\mathrm{x}_{m_1}, \mathrm{y}_{m_1}, \mathrm{t}_{p_1}; \theta)\Big)\,\mathrm{d}\mu \\ &= -\pi\left(A_m\frac{\omega_0}{\mathrm{c}}\right)^2\left[J_2\left(\frac{\omega_0}{\mathrm{c}}\mathrm{r}_{m_2,m_1}\right)\right. \\ &\quad\cdot\cos(2\phi_{m_2,m_1} - \theta_{m_1} - \theta_{m_2}) \\ &\quad\left. - J_0\left(\frac{\omega_0}{\mathrm{c}}\mathrm{r}_{m_2,m_1}\right)\cos(\theta_{m_2} - \theta_{m_1})\right] \\ &\quad\cdot\cos(\omega_0(\mathrm{t}_{p_2} - \mathrm{t}_{p_1})) \\ &\quad \forall n_1 \coloneqq (m_1, p_1), n_2 \coloneqq (m_2, p_2) \in \{(1,1),\dots,(M, P_M)\},\end{aligned} \tag{A·15}$$

respectively, from the following properties for Bessel functions of the first kind [37]:

$$\int_{\theta\in[0,2\pi)} \exp(\mathrm{i}z\cos\theta + \mathrm{i}\nu\theta)\,\mathrm{d}\mu = 2\pi\mathrm{i}^\nu J_\nu(z) \quad \forall z \in \mathbb{R}, \tag{A·16}$$

$$J_{-\nu}(z) = (-1)^\nu J_\nu(z) \quad \forall z \in \mathbb{R}, \tag{A·17}$$

where ν is an arbitrary integer.

Finally, the interchangeability of the integral and partial derivative in Eq. (A·10) is proved as follows. First, let $u \in \mathcal{U}$ and $\mathring{u} : [0, 2\pi) \to \mathbb{C}$ satisfy $u = \mathfrak{H}\mathring{u}$. Furthermore, for arbitrary fixed $y, t \in \mathbb{R}$, let $\varphi_X, u_X, \tilde{u}_X$ be respectively defined as

$$\varphi_X(x, \theta) \coloneqq \frac{\partial}{\partial x}\varphi(x, y, t; \theta) \quad \forall x \in \mathbb{R}, \theta \in [0, 2\pi), \tag{A·18}$$

$$u_X(x) \coloneqq \frac{\partial}{\partial x}u(x, y, t) \quad \forall x \in \mathbb{R}, \tag{A·19}$$

$$\tilde{u}_X(x) \coloneqq \int_{\theta\in[0,2\pi)} \mathrm{Re}\,(\mathring{u}(\theta)\varphi_x(x, \theta))\,\mathrm{d}\mu \quad \forall x \in \mathbb{R}. \tag{A·20}$$

Then, for arbitrary $x \in \mathbb{R}$, Cauchy's inequality yields the following relation:

$$\begin{aligned}&|\tilde{u}_X(x+h) - \tilde{u}_X(x)| \\ &= \left|\int_{\theta\in[0,2\pi)} \mathrm{Re}\,(\mathring{u}(\theta)(\varphi_X(x + h, \theta) - \varphi_X(x, \theta))\,\mathrm{d}\mu\right| \\ &\le \left(\int_{\theta\in[0,2\pi)} |\mathring{u}(\theta)|^2\,\mathrm{d}\mu\right. \\ &\quad\left.\cdot\int_{\theta\in[0,2\pi)} |\varphi_X(x + h, \theta) - \varphi_X(x, \theta)|^2\,\mathrm{d}\mu\right)^{\frac{1}{2}}.\end{aligned} \tag{A·21}$$

Since $\varphi_X(x+h, \theta)$ converges to $\varphi_X(x, \theta)$ as $h \to 0$ uniformly in $\theta \in [0, 2\pi)$, we obtain

$$\lim_{h\to 0} |\tilde{u}_X(x+h) - \tilde{u}_X(x)| = 0 \quad \forall x \in \mathbb{R}. \tag{A·22}$$

On the other hand, from the mean value theorem, for any $h \in \mathbb{R} \setminus \{0\}$, there exists some $\vartheta(h) \in [0, 1]$ satisfying

$$\frac{\varphi(x+h, y, t; \theta) - \varphi(x, y, t; \theta)}{h} = \varphi_X(x + \vartheta(h)h, \theta). \tag{A·23}$$

Therefore, we obtain

$$\begin{aligned} & u_X(x, y, t) \\ &= \lim_{h\to 0} \frac{1}{h} \int_{\theta\in[0,2\pi)} \mathrm{Re}(\mathring{u}(\theta)(\varphi(x+h, y, t; \theta) \\ &\qquad\qquad - \varphi(x, y, t; \theta))) \, \mathrm{d}\mu \\ &= \lim_{h\to 0} \int_{\theta\in[0,2\pi)} \mathrm{Re}\left(\mathring{u}(\theta)\varphi_X(x + \vartheta(h)h, \theta)\right) \mathrm{d}\mu \\ &= \lim_{h\to 0} \tilde{u}_X(x + \vartheta(h)h) \\ &= \tilde{u}_X(x) \quad \forall x \in \mathbb{R}. \end{aligned} \tag{A·24}$$

The same property also holds for a partial derivative with respect to y. Thus, we obtain the interchangeability of the integral and partial derivative in Eq. (A· 10).

Natsuki Ueno received the B.E. degree in engineering from Kyoto University, Kyoto, Japan, in 2016, and the M.S. and Ph.D. degrees in information science and technology from the University of Tokyo, Tokyo, Japan, in 2018 and 2021, respectively. He is currently a Project Assistant Professor at Tokyo Metropolitan University, Tokyo, Japan. His research interests include spatial audio and acoustic signal processing.

Shoichi Koyama received the B.E., M.S., and Ph.D. degrees from the University of Tokyo, Tokyo, Japan, in 2007, 2009, and 2014, respectively. In 2009, he was a Researcher in acoustic signal processing with the Nippon Telegraph and Telephone Corporation. He moved to the University of Tokyo in 2014, and since 2018, he has been an Assistant Professor (Lecturer). From 2016 to 2018, he was also a Visiting Researcher and JSPS overseas research fellow with Paris Diderot University (Paris7), Institut Langevin, Paris, France. His research interests include acoustic inverse problems, sound field analysis and synthesis, and spatial audio. He is a member of the Acoustical Society of America, the Audio Engineering Society, the Institute of Electronics, Information and Communication Engineers, and the Acoustical Society of Japan (ASJ). He was the recipient of Itakura Prize Innovative Young Researcher Award by ASJ in 2015, and the Research Award by Funai Foundation for Information Technology in 2018.

Hiroshi Saruwatari received the B.E., M.E., and Ph.D. degrees from Nagoya University, Japan, in 1991, 1993, and 2000, respectively. He joined SECOM IS Laboratory, Japan, in 1993, and Nara Institute of Science and Technology, Japan, in 2000. From 2014, he is currently a Professor of The University of Tokyo, Japan. His research interests include statistical audio signal processing, blind source separation (BSS), and speech enhancement. He has put his research into the world's first commercially available Independent-Component-Analysis-based BSS microphone in 2007. He received paper awards from IEICE in 2001 and 2006, from TAF in 2004, 2009, 2012, and 2018, from IEEE-IROS2005 in 2006, and from APSIPA in 2013 and 2018. He received DOCOMO Mobile Science Award in 2011, Ichimura Award in 2013, The Commendation for Science and Technology by the Minister of Education in 2015, Achievement Award from IEICE in 2017, and Hoko-Award in 2018. He has been professionally involved in various volunteer works for IEEE, EURASIP, IEICE, and ASJ. He is an APSIPA Distinguished Lecturer from 2018.